

## Folding of an Artificial $\beta$ -Sheet in Competitive Solvents

Elena Junquera<sup>†</sup> and James S. Nowick<sup>\*§</sup>

Department of Chemistry, University of California, Irvine,  
Irvine, California 92697-2025

Received September 14, 1998

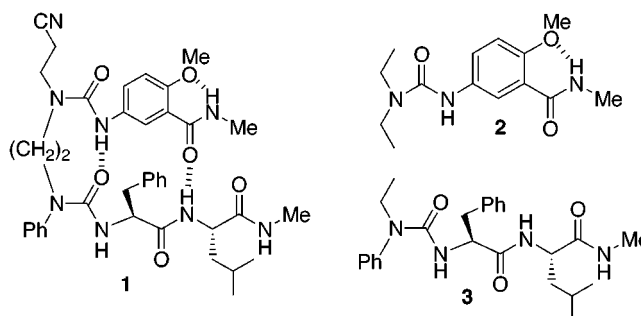
### Introduction

For the past few years, our research group has been developing and studying chemical models of protein  $\beta$ -sheets in which molecular templates induce  $\beta$ -sheetlike hydrogen bonding in attached peptide strands.<sup>1</sup> Through these studies, we have sought to gain an enhanced understanding of  $\beta$ -sheet structure and to develop biologically active peptidomimetic compounds.<sup>2</sup> Thus far, we have established that our model compounds fold into  $\beta$ -sheetlike structures in chloroform, a solvent that does not competitively bind to hydrogen-bonding groups within the molecules. Although noncompetitive solvents mimic the nonpolar environment that  $\beta$ -sheets experience in the interior of proteins, proteins fold in water. For this reason, it is important to study the structures of these compounds in water and other competitive solvents, as well as in chloroform. This paper describes our first studies of one of these artificial  $\beta$ -sheets in competitive solvents.

A few other research groups have already developed artificial  $\beta$ -sheets that fold in competitive solvents. Beginning in the mid 1980s, Feigel and co-workers published a series of papers in which molecular templates stabilize  $\beta$ -sheet structure in cyclopeptides, both in chloroform and in dimethyl sulfoxide solution. Feigel's templates are rigid tricyclic molecules that mimic a  $\beta$ -turn and hold peptide groups in proximity, thus inducing  $\beta$ -sheet formation.<sup>3</sup> Shortly thereafter, Kemp and co-workers developed a system in which a rigid tetracyclic molecule, which mimics the hydrogen-bonding functionality of a peptide in a  $\beta$ -strand conformation, templates  $\beta$ -sheet structure in adjacent peptide strands.<sup>4,5</sup> This system adopts a  $\beta$ -sheet conformation in both dimethyl

sulfoxide and in aqueous solution. Kelly and co-workers then reported a system in which a tricyclic template holds two peptide strands in proximity to induce  $\beta$ -sheet formation in aqueous solution.<sup>6</sup> In this system, hydrophobic interactions between the template and the peptide side-chains are essential in stabilizing the  $\beta$ -sheet structure. Within the past few years, a couple of other  $\beta$ -sheet systems that fold in competitive solvents have been reported.<sup>7,8</sup>

In 1996, we reported that compound **1** adopts a  $\beta$ -sheetlike structure in chloroform solution.<sup>1f</sup> In this compound, a 1,2-diaminoethane diurea turn unit holds a 5-amino-2-methoxybenzamide template next to a dipeptide strand; the 5-amino-2-methoxybenzamide template hydrogen bonds to the dipeptide strand, while the leucine side-chain packs against the aromatic ring of the 5-amino-2-methoxybenzamide template. In the current study, we set out to determine how well **1** retains this structure in competitive solvents by challenging **1** with methanol, 50% (v/v) aqueous methanol, and dimethyl sulfoxide.



### Results and Discussion

Our previous <sup>1</sup>H NMR studies established that **1** adopts the conformation shown in Figure 1 in chloroform solution.<sup>1f</sup> Evidence for this conformation included an

(4) (a) Kemp, D. S.; Bowen, B. R. *Tetrahedron Lett.* **1988**, 29, 5077. (b) Kemp, D. S.; Bowen, B. R. *Tetrahedron Lett.* **1988**, 29, 5081. (c) Kemp, D. S.; Bowen, B. R.; Muendel, C. C. *J. Org. Chem.* **1990**, 55, 4650.

(5) (a) Kemp, D. S.; Bowen, B. R. In *Protein Folding: Deciphering the Second Half of the Genetic Code*; Gierasch, L. M., King, J., Eds.; American Association for the Advancement of Science: Washington, DC, 1990; pp 293–303. (b) Kemp, D. S.; Muendel, C. C.; Blanchard, D. E.; Bowen, B. R. In *Peptides: Chemistry, Structure and Biology: Proceedings of the Eleventh American Peptide Symposium*; Rivier, J. E., Marshall, G. R., Eds.; ESCOM: Leiden, 1990; pp 674–676. (c) Kemp, D. S.; Blanchard, D. E.; Muendel, C. C. In *Peptides: Chemistry, Structure and Biology: Proceedings of the Twelfth American Peptide Symposium*; Smith, J. A., Rivier, J. E., Eds.; ESCOM: Leiden, 1992; pp 319–322.

(6) (a) Diaz, H.; Tsang, K. Y.; Choo, D.; Espina, J. R.; Kelly, J. W. *J. Am. Chem. Soc.* **1993**, 115, 3790. (b) Diaz, H.; Tsang, K. Y.; Choo, D.; Kelly, J. W. *Tetrahedron* **1993**, 49, 3533. (c) Tsang, K. Y.; Diaz, H.; Graciani, N.; Kelly, J. W. *J. Am. Chem. Soc.* **1994**, 116, 3988.

(7) (a) Kemp, D. S.; Li, Z. Q. *Tetrahedron Lett.* **1995**, 36, 4175. (b) Kemp, D. S.; Li, Z. Q. *Tetrahedron Lett.* **1995**, 36, 4179. (c) Schneider, J. P.; Kelly, J. W. *J. Am. Chem. Soc.* **1995**, 117, 2533. (d) Nesloney, C. L.; Kelly, J. W. *J. Am. Chem. Soc.* **1996**, 118, 5836. (e) The following paper claims to report a model for a parallel  $\beta$ -sheet but fails to provide adequate evidence for the proposed structure and appears to be in error: Gretchikhine, A. B.; Ogawa, M. Y. *J. Am. Chem. Soc.* **1996**, 118, 1543.

(8) A number of researchers have developed polypeptides that fold into  $\beta$ -sheet structures without the aid of synthetic molecular templates. For recent reviews, see: (a) Blanco, F.; Ramirez-Alvarado, M.; Serrano, L. *Curr. Opin. Struct. Biol.* **1998**, 8, 107. (b) Gellman, S. H. *Curr. Opin. Chem. Biol.* **1998**, 2, 717.

<sup>†</sup> Departamento de Quimica Fisica I, Facultad de Ciencias Quimicas, Universidad Complutense, 28040-Madrid, Spain.

<sup>§</sup> jsnwick@uci.edu.

(1) (a) Nowick, J. S.; Powell, N. A.; Martinez, E. J.; Smith, E. M.; Noronha, G. *J. Org. Chem.* **1992**, 57, 3763. (b) Nowick, J. S.; Powell, N. A.; Nguyen, T. M.; Noronha, G. *J. Org. Chem.* **1992**, 57, 7364. (c) Nowick, J. S.; Abdi, M.; Bellamo, K. A.; Love, J. A.; Martinez, E. J.; Noronha, G.; Smith, E. M.; Ziller, J. W. *J. Am. Chem. Soc.* **1995**, 117, 89. (d) Nowick, J. S.; Smith, E. M.; Noronha, G. *J. Org. Chem.* **1995**, 60, 7386. (e) Nowick, J. S.; Mahrus, S.; Smith, E. M.; Ziller, J. W. *J. Am. Chem. Soc.* **1996**, 118, 1066. (f) Nowick, J. S.; Holmes, D. L.; Mackin, G.; Noronha, G.; Shaka, A. J.; Smith, E. M. *J. Am. Chem. Soc.* **1996**, 118, 2764. (g) Nowick, J. S.; Holmes, D. L.; Noronha, G.; Smith, E. M.; Nguyen, T. M.; Huang, S.-L. *J. Org. Chem.* **1996**, 61, 3929. (h) Nowick, J. S.; Pairish, M.; Lee, I. Q.; Holmes, D. L.; Ziller, J. W. *J. Am. Chem. Soc.* **1997**, 119, 5413. (i) Holmes, D. L.; Smith, E. M.; Nowick, J. S. *J. Am. Chem. Soc.* **1997**, 119, 7665. (j) Nowick, J. S.; Insaf, S. *J. Am. Chem. Soc.* **1997**, 119, 10903. (k) Smith, E. M.; Holmes, D. L.; Shaka, A. J.; Nowick, J. S. *J. Org. Chem.* **1997**, 62, 7906.

(2) For reviews, see: (a) Nowick, J. S.; Smith, E. M.; Pairish, M. *Chem. Soc. Rev.* **1996**, 25, 401. (b) Nowick, J. S. *Chem. Br.* **1997**, 33 (12), 36. (c) Nowick, J. S. *Acc. Chem. Res.*, in press.

(3) (a) Feigel, M. *J. Am. Chem. Soc.* **1986**, 108, 181. (b) Wagner, G.; Feigel, M. *Tetrahedron* **1993**, 49, 10831. (c) Brandmeier V.; Sauer, W. H. B.; Feigel M. *Helv. Chim. Acta* **1994**, 77, 70.

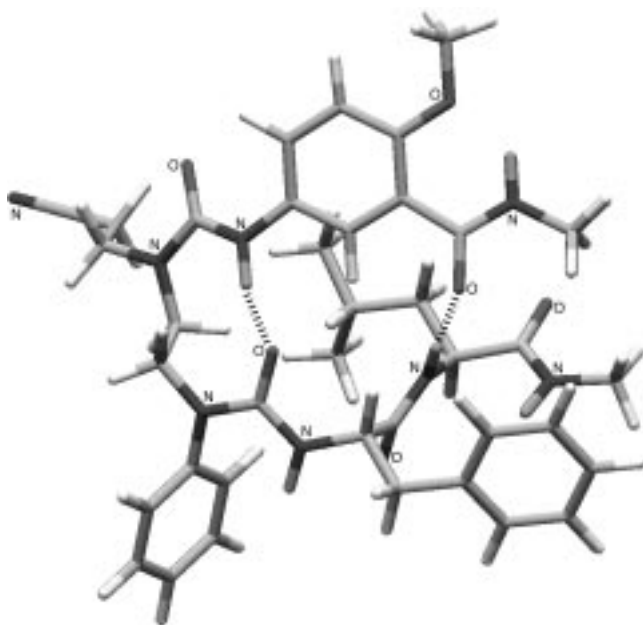


**Figure 1.** Model illustrating the structure of **1** in  $\text{CDCl}_3$  solution. (For details, see ref 1f.)

extensive network of NOEs between the 5-amino-2-methoxybenzamide template and the dipeptide strand, downfield shifting of the hydrogen-bonded NH groups relative to control compounds **2** and **3**, and upfield shifting of one of the leucine methyl groups in the  $^1\text{H}$  NMR spectrum. To determine the extent to which this structure is retained in competitive solvents, we have now examined NOEs and chemical shifts of key protons in four sets of solvents: chloroform ( $\text{CDCl}_3$ ), methanol ( $\text{CD}_3\text{OD}$  and  $\text{CD}_3\text{OH}$ ), aqueous methanol (50% v/v  $\text{CD}_3\text{OD}-\text{D}_2\text{O}$  and 50% v/v  $\text{CD}_3\text{OH}-\text{H}_2\text{O}$ ), and dimethyl sulfoxide ( $\text{CD}_3\text{SOCD}_3$ ). The hydroxylic solvents (methanol and 50% aqueous methanol) were used in partially deuterated form ( $\text{CD}_3\text{OH}$  and 50% v/v  $\text{CD}_3\text{OH}-\text{H}_2\text{O}$ ), to permit the observation of NH resonances with solvent-suppression techniques, and in fully deuterated form ( $\text{CD}_3\text{OD}$  and 50% v/v  $\text{CD}_3\text{OD}-\text{D}_2\text{O}$ ), to facilitate the observation of all other resonances while minimizing artifacts associated with suppression of the hydroxylic resonances.<sup>9</sup> Nuclear Overhauser effect studies were performed using the transverse ROESY (Tr-ROESY) method,<sup>10</sup> because **1** has a molecular weight of 713 and exhibits NOEs at 500 MHz that range from small and positive (in chloroform and methanol), to near zero (in aqueous methanol), to small and negative (in dimethyl sulfoxide).

Interstrand NOEs provide compelling evidence for long-range order in  $\beta$ -sheet structures. In  $\text{CDCl}_3$  solution, artificial  $\beta$ -sheet **1** exhibits NOEs between the 6-position of the aromatic ring of the  $\beta$ -strand mimic and the phenylalanine  $\alpha$ -proton, the leucine NH proton, and the leucine side-chain (Figure 2). In this solvent, artificial  $\beta$ -sheet **1** also exhibits NOEs between the methylamide methyl group of the  $\beta$ -strand mimic and the leucine NH

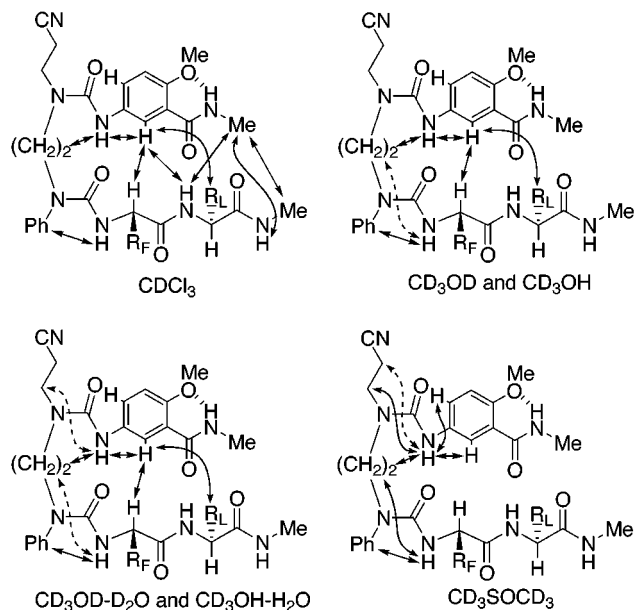


**Figure 2.** Key NOEs detected by Tr-ROESY studies of artificial  $\beta$ -sheet **1** in chloroform, methanol, aqueous methanol, and dimethyl sulfoxide. Interstrand NOEs are shown with arrows between the upper and lower halves of the molecule. Short-range NOEs involving the urea groups are shown with arrows to these groups; dotted arrows represent short-range NOEs that are relatively weak.

and methylamide groups. Fewer interstrand NOEs are present in methanol and methanol–water mixtures, with NOEs seen between the 6-position of the aromatic ring of the  $\beta$ -strand mimic and the phenylalanine  $\alpha$ -proton and the leucine side-chain.<sup>11</sup> No interstrand NOEs are seen in dimethyl sulfoxide. These interstrand NOEs indicate that artificial  $\beta$ -sheet **1** is well-structured (folded) in chloroform, partially structured in methanol and methanol–water mixtures, and unstructured (unfolded) in dimethyl sulfoxide.

In dimethyl sulfoxide, **1** exhibits many NOEs in violation of the  $\beta$ -sheet structure. Most notably, the “upper” urea NH exhibits NOEs with both the 1,2-diaminoethane and cyanoethyl groups of the turn unit (Figure 2). The NOEs with the  $\text{CH}_2\text{CH}_2\text{CN}$  protons are of comparable intensities to those with the  $\text{NCH}_2\text{CH}_2\text{N}$  protons, while those with the  $\text{CH}_2\text{CH}_2\text{CN}$  protons (represented by dashed arrows in Figure 2) are weaker. The magnitudes of the NOEs to the cyanoethyl group suggest that there is little conformational bias about the  $\text{R}_2\text{N}-\text{CO}$  bond of the upper urea group. The upper urea NH also exhibits NOEs with both the 4- and the 6-positions of the aromatic ring of the  $\beta$ -strand mimic. These NOEs are of comparable strength, indicating that there is little or no conformational bias about the  $\text{N}-\text{Ar}$  bond of the  $\beta$ -strand mimic.<sup>12</sup> Similarly, the “lower” urea NH (phenylalanine NH) exhibits NOEs with both the phenyl group of the turn unit (PhN) and the diaminoethane group ( $\text{NCH}_2\text{CH}_2\text{N}$ ), suggesting that rotation occurs about the

(9) The  $\text{H}_2\text{O}$  in the 50% v/v  $\text{CD}_3\text{OH}-\text{H}_2\text{O}$  mixture was buffered to pH 5.0 to reduce the rate of exchange of NH protons: Wüthrich, K. *NMR of Proteins and Nucleic Acids*; Wiley: New York, 1986; pp 23–25.

(10) (a) Hwang, T. L.; Shaka, A. J. *J. Am. Chem. Soc.* **1992**, *114*, 3157. (b) Hwang, T. L.; Shaka, A. J. *J. Magn. Reson. Ser. B* **1993**, *102*, 155.

(11) An NOE between the methylamide methyl group of the  $\beta$ -strand mimic and the leucine methylamide methyl group may be present in aqueous methanol but could not be established with certainty because of the proximity of their resonances ( $\Delta\delta = 0.30$  ppm) and their large noise ridges in the Tr-ROESY spectrum.

(12) In the model shown in Figure 1, the upper urea NH is 2.3 Å from  $\text{H}_6$  of the aromatic ring of the  $\beta$ -strand mimic and 3.7 Å from  $\text{H}_4$ . The former distance should give rise to a strong NOE, while the latter should give rise to a much weaker NOE.

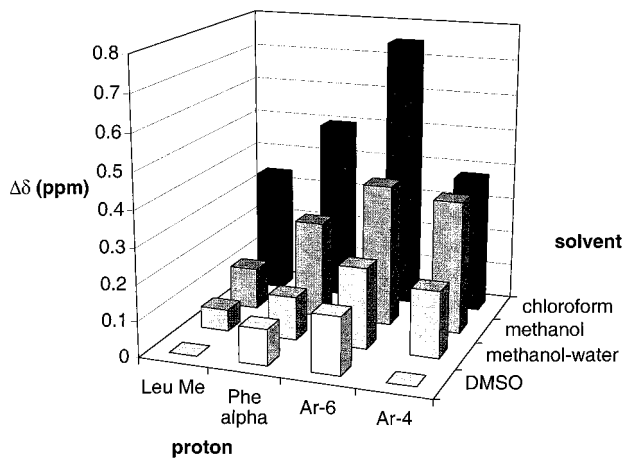


**Figure 3.** Chemical shift differences between key protons of artificial  $\beta$ -sheet **1** and controls **2** and **3** in various solvents: (a) separation of the leucine methyl groups of **1**, (b) chemical shift difference between the phenylalanine  $\alpha$ -protons of **1** and **3**, (c) chemical shift difference between  $H_6$  of the 5-amino-2-methoxybenzamide templates of **1** and **2**, (d) chemical shift difference between  $H_4$  of the 5-amino-2-methoxybenzamide templates of **1** and **2**.

Ph(R)N–CO bond of the lower urea group. In aqueous methanol, these inconsistent NOEs are weaker and fewer (dashed arrows in Figure 2), and no NOE is observed between the upper urea NH and the  $\text{CH}_2\text{CH}_2\text{CN}$  protons. In methanol, no inconsistent NOEs involving the upper urea are observed, and the inconsistent NOEs involving the lower urea are weak. In chloroform, the urea groups show no inconsistent NOEs: the upper urea NH group exhibits NOEs with the 1,2-diaminoethane group but not with the cyanoethyl group; the lower urea NH exhibits NOEs with the phenyl group of the turn unit but not with the diaminoethane group. These observations suggest that rotation about the urea groups is restricted in chloroform, occurs freely in dimethyl sulfoxide, and is partially restricted in methanol and aqueous methanol.

The chemical shifts of various protons in **1** provide additional evidence for its structure. In  $\text{CDCl}_3$  solution, one of the leucine methyl resonances of **1** appears shifted upfield at 0.45 ppm, while the other appears at 0.79 ppm. This upfield shifting and large (0.34 ppm) separation between the resonances occur because the *pro-R* methyl group of **1** sits over the face of the 5-amino-2-methoxybenzamide template.<sup>13</sup> In the more competitive solvents, the methyl resonances are less separated: 0.12 ppm in methanol, 0.06 ppm in methanol–water, and 0.00 ppm in dimethyl sulfoxide.<sup>13</sup> Figure 3 illustrates these data graphically. The decreasing differentiation of the methyl groups parallels the trends among the NOE data and reflects a decrease in structure across this series of solvents.

The diastereotopic leucine  $\beta$ -protons exhibit comparable trends in differentiation, with separations of 0.47 ppm in chloroform, 0.06 ppm in methanol,  $\sim 0.03$  ppm in aqueous methanol, and 0.00 ppm in dimethyl sulfoxide.<sup>14</sup> The diastereotopic protons associated with the turn unit ( $\text{NCH}_2\text{CH}_2\text{N}$  and  $\text{NCH}_2\text{CH}_2\text{CN}$ ) behave similarly, ap-

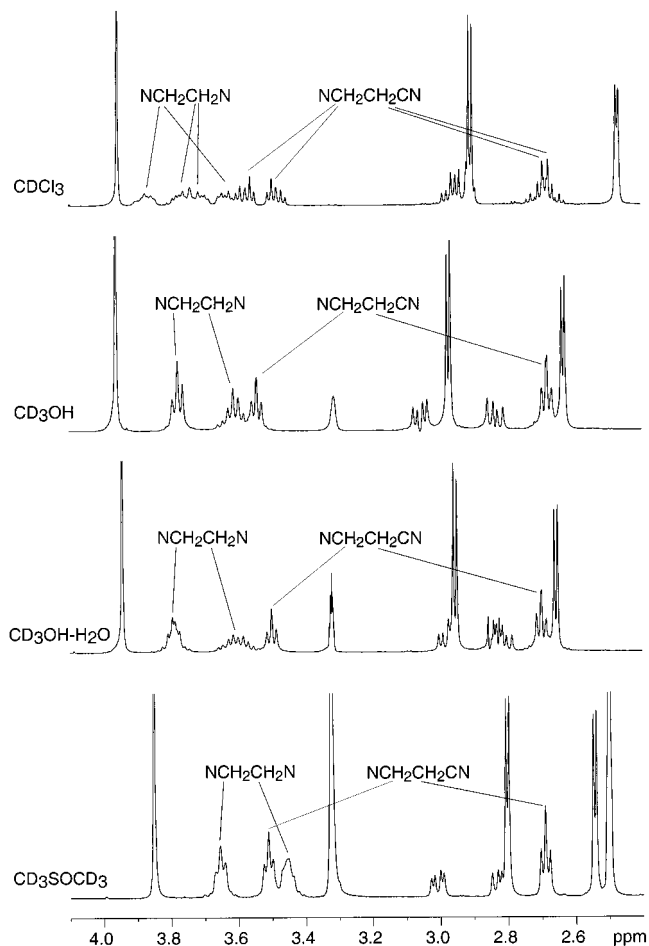


**Figure 4.**  $^1\text{H}$  NMR spectra of artificial  $\beta$ -sheet **1** in  $\text{CDCl}_3$ ,  $\text{CD}_3\text{OH}$ ,  $\text{CD}_3\text{OH}-\text{H}_2\text{O}$ , and  $\text{CD}_3\text{SOCD}_3$ , illustrating splitting of diastereotopic methylene protons of the turn unit ( $\text{NCH}_2\text{CH}_2\text{N}$  and  $\text{NCH}_2\text{CH}_2\text{CN}$ ).

pearing as eight resolved multiplets (1 H each) in chloroform and as four triplets and near triplets (2 H each) in dimethyl sulfoxide (Figure 4). In methanol and aqueous methanol these protons exhibit slightly more splitting, appearing as four near triplets and more complex multiplets (2 H each).<sup>15</sup>

The chemical shift of the phenylalanine  $\alpha$ -proton of **1** provides another index of  $\beta$ -sheet structure and follows the trend shown by the chemical shift and NOE data described above. The chemical shift of an  $\alpha$ -proton of an amino acid in a  $\beta$ -sheet is generally several tenths of a ppm downfield of the same residue in a random coil.<sup>16</sup> Comparison of the chemical shift of the phenylalanine

(13) The leucine methyl groups of control **3** show no analogous trend in chemical shifts, with shift differences of 0.02–0.06 ppm in the various solvents.

(14) The diastereotopic leucine  $\beta$ -protons of control **3** are separated by 0.00–0.03 ppm in the various solvents.

(15) The  $^3J_{\text{HH}}$  coupling constants of the leucine side-chain reflect its conformation and parallel the trend of decreasing structure across the series of solvents. In  $\text{CDCl}_3$ , the  $\alpha\beta$  and  $\alpha\beta'$  coupling constants differ substantially, as do the  $\beta\gamma$  and  $\beta'\gamma$  coupling constants ( $J_{\alpha\beta} = 3$  Hz,  $J_{\alpha\beta'} = 12$  Hz,  $J_{\beta\gamma} = 12$  Hz,  $J_{\beta'\gamma} = 3$  Hz). These coupling constants reflect Karplus relationships associated with  $60^\circ$  and  $180^\circ$  dihedral angles between the protons and indicate that a single side-chain conformation predominates (shown in Figure 1). In methanol and methanol–water, the coupling constants are less differentiated (methanol:  $J_{\alpha\beta} = 5$  Hz,  $J_{\alpha\beta'} = 11$  Hz,  $J_{\beta\gamma} = 9$  Hz,  $J_{\beta'\gamma} = 5$  Hz; methanol–water:  $J_{\alpha\beta} = 5$  Hz,  $J_{\alpha\beta'} = 10$  Hz). (The coupling constants  $J_{\beta\gamma}$  and  $J_{\beta'\gamma}$  could not be determined in methanol–water, because the leucine  $\beta$ ,  $\beta'$ , and  $\gamma$  resonances overlap.) In dimethyl sulfoxide, the coupling constants are not differentiated ( $J_{\alpha\beta} = J_{\alpha\beta'} = 8$  Hz,  $J_{\beta\gamma} = J_{\beta'\gamma} = 7$  Hz), reflecting the absence of a significant conformational preference of the side-chain. (The  $J_{\alpha\beta}$  and  $J_{\alpha\beta'}$  coupling constants for the phenylalanine side-chain are 5–7 Hz and 8–10 Hz in all of the solvents, indicating that it is not conformationally ordered.)

$\alpha$ -proton of **1** to that of control **3** reveals shift differences of 0.50, 0.27, 0.12, and 0.10 ppm, respectively, in chloroform, methanol, methanol-water, and dimethyl sulfoxide. These data are shown graphically in Figure 3 and are consistent with a model in which the degree of  $\beta$ -sheet structure decreases across the series of solvents. No significant differences between the chemical shifts of the leucine  $\alpha$ -protons of **1** and **3** are seen ( $\leq 0.02$  ppm). The absence of a trend for this residue may reflect that it extends beyond the hydrogen-bonded  $\beta$ -sheet structure and is not really part of the  $\beta$ -sheet.

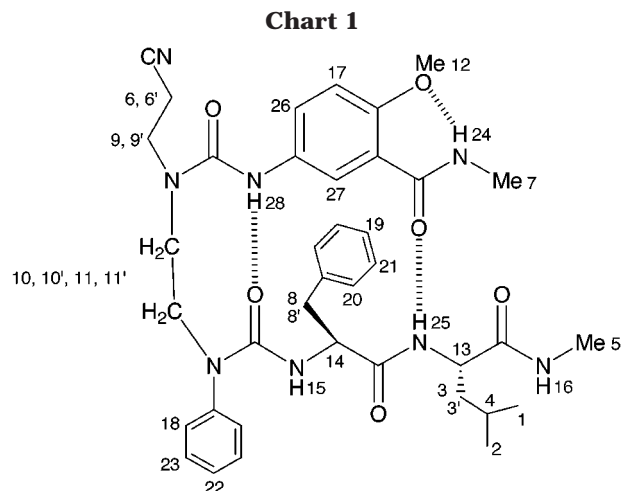
The chemical shifts of the protons at the 4- and 6-positions of the 5-amino-2-methoxybenzamide template follow the same trend. The differences in shift between  $H_6$  of artificial  $\beta$ -sheet **1** and control **3** are 0.75, 0.40, 0.23, and 0.16 across the series of solvents (Figure 3). The differences in shift between  $H_4$  of **1** and **3** are 0.38, 0.37, 0.19, and  $-0.01$  (Figure 3). The downfield shifting of  $H_4$  and  $H_6$  is analogous to the downfield shifting of  $\alpha$ -protons in  $\beta$ -sheets and probably reflects their enforced proximity to carbonyl groups in the folded conformation of **1**.<sup>17</sup>

### Conclusion

The NOE and chemical shift studies described herein show that artificial  $\beta$ -sheet **1** is partially folded in methanol and aqueous methanol solutions. The degree of folding decreases across the series of solvents studied, ranging from well-structured in chloroform to relatively unstructured in dimethyl sulfoxide and following the trend chloroform > methanol > methanol-water > dimethyl sulfoxide. These findings are significant, because they establish that the diurea turn unit and the 5-amino-2-methoxybenzamide template can induce  $\beta$ -sheet structure in an attached peptide strand in competitive protic solvents. In future studies, we plan to exploit this finding by developing artificial  $\beta$ -sheets that are water soluble and fold in pure water. The current study lays the groundwork for these plans.

### Experimental Section

NMR studies were performed at 25 °C on a Bruker DRX500 spectrometer using 10 mM samples of **1–3** in CDCl<sub>3</sub>, CD<sub>3</sub>OD, CD<sub>3</sub>OH, 50% v/v CD<sub>3</sub>OD–D<sub>2</sub>O, 50% v/v CD<sub>3</sub>OH–H<sub>2</sub>O, and CD<sub>3</sub>SOCD<sub>3</sub>. The H<sub>2</sub>O in the 50% v/v CD<sub>3</sub>OH–H<sub>2</sub>O mixture was buffered to pH 5.0 with 0.04 M CD<sub>3</sub>CO<sub>2</sub>D/CD<sub>3</sub>CO<sub>2</sub>Na.<sup>9</sup> Tetramethylsilane (TMS) was used as a reference in the organic solvents, and sodium 3-(trimethylsilyl)propanesulfonate was used as a reference in the aqueous methanol solutions. All the samples were sealed under vacuum after 5–7 freeze–pump–thaw degassing cycles on a high-vacuum line (<0.001 mmHg), with the exception of those in CD<sub>3</sub>OH–H<sub>2</sub>O and CD<sub>3</sub>SOCD<sub>3</sub>, which were not degassed. COSY spectra were recorded using standard pulsed field gradient (PFG) techniques.<sup>18</sup> ROESY spectra were recorded with a mixing time of 300 ms using the Tr-ROESY pulse sequence of Hwang and Shaka.<sup>10</sup> A spin locking field strength of 5 kHz was employed to collect 2048 points in the  $f_2$  dimension and 512 points in the  $f_1$  dimension, a relaxation delay of 1 s was used, and 24 transients were collected for each  $t_1$  value. For experiments involving CD<sub>3</sub>OH and CD<sub>3</sub>OH–H<sub>2</sub>O, solvent suppression was performed by appending the pulsed field gradient technique of Shaka and Hwang<sup>19</sup> to the end of the pulse sequence. The data were processed using Bruker XWINNMR



software. A sine-squared window function shifted by 60° was applied in both dimensions, and forward linear prediction of 1024 points was performed in the  $f_1$  dimension to give a final matrix of 1024 by 512 real points. An automatic baseline correction was applied in both dimensions after Fourier transforming the data. <sup>1</sup>H NMR resonances were assigned by a combination of one-dimensional and two-dimensional (PFG COSY and Tr-ROESY) methods. These assignments are shown in Chart 1 and are listed in the spectral summaries that follow.

**<sup>1</sup>H NMR Data for Artificial  $\beta$ -Sheet 1 in CDCl<sub>3</sub>.**  $\delta$  0.45 (d,  $J = 6.3$  Hz, 3 H, 1), 0.79 (d,  $J = 6.2$  Hz, 3 H, 2), 1.11 (td,  $J = 12.3, 3.2$  Hz, 1 H, 3), 1.57 (td,  $J = 11.8, 3.6$  Hz, 1 H, 3'), 1.47–1.55 (m, 1 H, 4), 2.47 (d,  $J = 4.1$  Hz, 3 H, 5), 2.66 (dt,  $J = 17.0, 6.3$  Hz, 1 H, 6), 2.71 (dt,  $J = 17.0, 6.3$  Hz, 1 H, 6'), 2.91 (d,  $J = 4.8$  Hz, 3 H, 7), 2.91 (dd, ABX pattern,  $J_{AB} = 13.2$  Hz,  $J_{BX} = 10.3$  Hz, 1 H, 8), 2.97 (dd, ABX pattern,  $J_{AB} = 13.2$  Hz,  $J_{AX} = 6.4$  Hz, 1 H, 8'), 3.48 (dt,  $J = 13.8, 6.4$  Hz, 1 H, 9), 3.57 (dt,  $J = 13.9, 6.2$  Hz, 1 H, 9'), 3.63 (appar ddd,  $J = 11.0, 5.5$  Hz, 1 H, 10), 3.67–3.74 (m, 1 H, 11), 3.74–3.82 (m, 1 H, 11'), 3.82–3.92 (m, 1 H, 10'), 3.95 (s, 3 H, 12), 4.39 (ddd,  $J = 12.1, 9.0, 3.4$  Hz, 1 H, 13), 4.94 (ddd,  $J = 10.1, 8.5, 6.6$  Hz, 1 H, 14), 5.03 (d,  $J = 8.5$  Hz, 1 H, 15), 5.49 (appar br s, 1 H, 16), 6.92 (d,  $J = 9.1$  Hz, 1 H, 17), 7.15 (appar d,  $J = 7.2$  Hz, 2 H, 18), 7.26–7.31 (m, 1 H, 19), 7.32 (appar d,  $J = 4.4$  Hz, 4 H, 20 and 21), 7.39 (appar t,  $J = 7.3$  Hz, 1 H, 22), 7.46 (appar t,  $J = 7.8$  Hz, 2 H, 23), 8.10 (appar br q,  $J = 4.8$  Hz, 1 H, 24), 8.20 (d,  $J = 9.0$  Hz, 1 H, 25), 8.37 (dd,  $J = 9.0, 2.8$  Hz, 1 H, 26), 8.53 (d,  $J = 2.9$  Hz, 1 H, 27), 10.0 (s, 1 H, 28).

**<sup>1</sup>H NMR Data for Artificial  $\beta$ -Sheet 1 in CD<sub>3</sub>OD.**  $\delta$  0.70 (d,  $J = 6.6$  Hz, 3 H, 1), 0.81 (d,  $J = 6.5$  Hz, 3 H, 2), 1.41 (ddd,  $J = 13.6, 10.3, 5.1$  Hz, 1 H, 3), 1.47 (ddd,  $J = 13.8, 9.2, 5.0$  Hz, 1 H, 3'), 1.51–1.62 (m, 1 H, 4), 2.63 (s, 3 H, 5), 2.68 (appar td,  $J = 6.7, 1.8$  Hz, 2 H, 6 and 6'), 2.97 (s, 3 H, 7), 2.84 (dd, ABX pattern,  $J_{AB} = 13.8, J_{BX} = 8.6$  Hz, 1 H, 8), 3.06 (dd, ABX pattern,  $J_{AB} = 13.8, J_{AX} = 6.4$  Hz, 1 H, 8'), 3.54 (appar td,  $J = 6.6, 1.7$  Hz, 2 H, 9 and 9'), 3.57–3.66 (m, 2 H, 10 and 10'), 3.78 (appar t,  $J = 7.5$  Hz, 2 H, 11 and 11'), 3.96 (s, 3 H, 12), 4.33 (dd,  $J = 10.3, 4.9$  Hz, 1 H, 13), 4.71 (dd,  $J = 8.5, 6.5$  Hz, 1 H, 14), 7.08 (d,  $J = 9.2$  Hz, 1 H, 17), 7.10–7.15 (m, 4 H, 18 and 20), 7.20–7.27 (m, 3 H, 19 and 21), 7.36 (appar tt,  $J = 7.3, 1.5$  Hz, 1 H, 22), 7.40–7.45 (m, 2 H, 23), 7.91 (dd,  $J = 9.0, 2.8$  Hz, 1 H, 26), 8.20 (d,  $J = 2.8$  Hz, 1 H, 27).

**<sup>1</sup>H NMR Data for Artificial  $\beta$ -Sheet 1 in CD<sub>3</sub>OH.**  $\delta$  0.70 (d,  $J = 6.8$  Hz, 3 H, 1), 0.82 (d,  $J = 6.7$  Hz, 3 H, 2), 1.41 (ddd,  $J = 13.7, 9.2, 4.9$  Hz, 1 H, 3), 1.47 (ddd,  $J = 13.7, 10.7, 5.2$  Hz, 1 H, 3'), 1.51–1.61 (m, 1 H, 4), 2.63 (d,  $J = 4.8$  Hz, 3 H, 5), 2.68 (appar td,  $J = 6.7, 1.2$  Hz, 2 H, 6 and 6'), 2.97 (d,  $J = 4.8$  Hz, 3 H, 7), 2.83 (dd, ABX pattern,  $J_{AB} = 14.3, J_{BX} = 8.5$  Hz, 1 H, 8), 3.06 (dd, ABX pattern,  $J_{AB} = 14.3, J_{AX} = 6.4$  Hz, 1 H, 8'), 3.54 (appar t,  $J = 7.5$  Hz, 2 H, 9 and 9'), 3.57–3.67 (m, 2 H, 10 and 10'), 3.78 (appar t,  $J = 7.8$  Hz, 2 H, 11 and 11'), 3.96 (s, 3 H, 12), 4.33 (ddd,  $J = 11.0, 8.5, 4.9$  Hz, 1 H, 13), 5.50 (d,  $J = 7.4$

(16) (a) Wishart, D. S.; Sykes, B. D.; Richards, F. M. *J. Mol. Biol.* **1991**, *222*, 311. (b) Wishart, D. S.; Sykes, B. D.; Richards, F. M. *Biochemistry* **1992**, *31*, 1647.

(17) Wagner, G.; Pardi, A.; Wüthrich, K. *J. Am. Chem. Soc.* **1983**, *105*, 5948.

(18) Hurd, R. E. *J. Magn. Reson.* **1990**, *87*, 422.

(19) Hwang, T. L.; Shaka, A. J. *J. Magn. Reson. Ser. A* **1995**, *112*, 275.

Hz, 1 H, 15), 7.08 (d,  $J = 9.4$  Hz, 1 H, 17), 7.10–7.17 (m, 4 H, 18 and 20), 7.20–7.29 (m, 3 H, 19 and 21), 7.35 (br s, 1 H, 16), 7.35–7.39 (m, 1 H, 22), 7.40–7.45 (m, 2 H, 23), 7.90 (dd,  $J = 9.0, 2.7$  Hz, 1 H, 26), 8.19 (d,  $J = 2.8$  Hz, 1 H, 27), 8.26 (d,  $J = 8.4$  Hz, 1 H, 25), 8.46 (appar q,  $J = 4.9$  Hz, 1 H, 24), 9.35 (s, 1 H, 28).

**$^1\text{H}$  NMR Data for Artificial  $\beta$ -Sheet 1 in 50% v/v  $\text{CD}_3\text{OD}-\text{D}_2\text{O}$ .**  $\delta$  0.73 (d,  $J = 5.9$  Hz, 3 H, 1), 0.79 (d,  $J = 5.9$  Hz, 3 H, 2), 1.35–1.52 (m, 3 H, 3, 3', and 4), 2.66 (s, 3 H, 5), 2.71 (appar td,  $J = 6.4, 1.5$  Hz, 2 H, 6 and 6'), 2.96 (s, 3 H, 7), 2.82 (dd, ABX pattern,  $J_{\text{AB}} = 13.7, J_{\text{BX}} = 8.3$  Hz, 1 H, 8), 2.99 (dd, ABX pattern,  $J_{\text{AB}} = 13.9, J_{\text{AX}} = 6.4$  Hz, 1 H, 8'), 3.51 (appar t,  $J = 6.6, 2$  H, 9 and 9'), 3.55–3.68 (m, 2 H, 10 and 10'), 3.75–3.85 (m, 2 H, 11 and 11'), 3.95 (s, 3 H, 12), 4.27 (dd,  $J = 9.8, 4.3$  Hz, 1 H, 13), 4.59 (dd,  $J = 8.0, 6.4$  Hz, 1 H, 14), 7.03–7.07 (m, 2 H, 20), 7.08–7.11 (appar d,  $J = 7.3$  Hz, 2 H, 18), 7.13 (d,  $J = 9.1$  Hz, 1 H, 17), 7.22–7.28 (m, 3 H, 19 and 21), 7.39–7.44 (appar t,  $J = 7.4$  Hz, 1 H, 22), 7.44–7.48 (appar t,  $J = 7.4$  Hz, 2 H, 23), 7.66 (dd,  $J = 8.9, 2.4$  Hz, 1 H, 26), 7.91 (d,  $J = 2.7$  Hz, 1 H, 27).

**$^1\text{H}$  NMR Data for Artificial  $\beta$ -Sheet 1 in 50% v/v  $\text{CD}_3\text{OH}-\text{H}_2\text{O}$ .**  $\delta$  0.73 (d,  $J = 6.1$  Hz, 3 H, 1), 0.78 (d,  $J = 6.0$  Hz, 3 H, 2), 1.37–1.52 (m, 3 H, 3, 3', and 4), 2.66 (d,  $J = 4.9$  Hz, 3 H, 5), 2.70 (appar td,  $J = 6.7, 1.2$  Hz, 2 H, 6 and 6'), 2.96 (d,  $J = 4.9$  Hz, 3 H, 7), 2.81 (dd, ABX pattern,  $J_{\text{AB}} = 14.0$  Hz,  $J_{\text{BX}} = 8.2$  Hz, 1 H, 8), 2.98 (appar dd, ABX pattern,  $J_{\text{AB}} = 14.2$  Hz,  $J_{\text{AX}} = 6.2$  Hz, 1 H, 8'), 3.50 (appar t,  $J = 6.7$  Hz, 2 H, 9 and 9'), 3.54–3.67 (m, 2 H, 10 and 10'), 3.74–3.86 (m, 2 H, 11 and 11'), 3.94 (s, 3 H, 12), 4.27 (appar ddd,  $J = 11.0, 8.5, 5.4$  Hz, 1 H, 13), 5.41 (d,  $J = 7.3$  Hz, 1 H, 15), 7.02–7.06 (m, 2 H, 20), 7.07–7.10 (appar d,  $J = 7.9$  Hz, 2 H, 18), 7.12 (d,  $J = 9.5$  Hz, 1 H, 17), 7.22–7.27 (m, 3 H, 19 and 21), 7.39–7.47 (m, 3 H, 22 and 23), 7.53 (appar q,  $J = 4.9$  Hz, 1 H, 16), 7.62 (dd,  $J = 9.5, 2.8$  Hz, 1 H, 26), 7.87 (d,  $J = 2.8$  Hz, 1 H, 27), 8.08 (d,  $J = 8.2$  Hz, 1 H, 25), 8.54 (appar q,  $J = 5.2$  Hz, 1 H, 24), 8.81 (s, 1 H, 28).

**$^1\text{H}$  NMR Data for Artificial  $\beta$ -Sheet 1 in  $\text{CD}_3\text{SOCD}_3$ .**  $\delta$  0.79 (d,  $J = 6.6$  Hz, 6 H, 1 and 2), 1.40 (appar t,  $J = 7.3$  Hz, 2 H, 3 and 3'), 1.47–1.57 (m, 1 H, 4), 2.54 (d,  $J = 4.6$  Hz, 3 H, 5), 2.69 (appar t,  $J = 6.8$  Hz, 2 H, 6 and 6'), 2.80 (d,  $J = 4.7$  Hz, 3 H, 7), 2.83 (dd, ABX pattern,  $J_{\text{AB}} = 13.7, J_{\text{BX}} = 5.0$  Hz, 1 H, 8), 3.01 (appar dd, ABX pattern,  $J_{\text{AB}} = 13.7, J_{\text{AX}} = 8.6$  Hz, 1 H, 8'), 3.42–3.48 (m, 2 H, 10 and 10'), 3.51 (appar t,  $J = 6.9$  Hz, 2 H, 9 and 9'), 3.61–3.71 (m, 2 H, 11 and 11'), 3.85 (s, 3 H, 12), 4.20 (appar q,  $J = 7.8$  Hz, 1 H, 13), 4.50 (appar ddd,  $J = 8.6, 7.9, 5.0$  Hz, 1 H, 14), 5.75 (d,  $J = 7.9$  Hz, 1 H, 15), 7.02 (d,  $J = 9.1$  Hz, 1 H, 17), 7.08–7.14 (m, 4 H, 18 and 20), 7.16–7.24 (m, 3 H, 19 and 21), 7.27–7.31 (m, 1 H, 22), 7.35–7.40 (m, 2 H, 23), 7.62 (dd,  $J = 8.9, 2.8$  Hz, 1 H, 26), 7.66 (appar q,  $J = 4.7$  Hz, 1 H, 16), 7.99 (d,  $J = 2.7$  Hz, 1 H, 27), 8.03 (d,  $J = 8.3$  Hz, 1 H, 25), 8.16 (appar q,  $J = 4.7$  Hz, 1 H, 24), 8.84 (s, 1 H, 28).

**Acknowledgment.** This work was supported by the National Institutes of Health (Grant GM-49076). E.J. thanks the Programa Del Amo of the Universidad Complutense of Madrid for financial support. J.S.N. thanks the following agencies for support in the form of awards: the National Science Foundation (Presidential Faculty Fellow Award), the Camille and Henry Dreyfus Foundation (Teacher-Scholar Award), and the Alfred P. Sloan Foundation (Alfred P. Sloan Research Fellowship).

**Supporting Information Available:** PFG COSY and Tr-ROESY spectra of artificial  $\beta$ -sheet 1 in  $\text{CDCl}_3$ ,  $\text{CD}_3\text{OD}$ ,  $\text{CD}_3\text{OH}$ , 50% v/v  $\text{CD}_3\text{OD}-\text{D}_2\text{O}$ , 50% v/v  $\text{CD}_3\text{OH}-\text{H}_2\text{O}$ , and  $\text{CD}_3\text{SOCD}_3$  solution (59 pages). This material is available free of charge via the Internet at <http://pubs.acs.org>.

JO9818576